Research Square

Preprints are preliminary reports that have not undergone peer review.
They should not be considered conclusive, used to inform clinical practice,
or referenced by the media as validated information.

Stable reconstruction of a spatial source term in a time-space fractional diffusion equation using Tikhonov regularization and final-time measurements

Ihya Talibi

ihya.talibi@usms.ma

FST Béni Mellal, Sultan Moulay Slimane University

Abdessamad Oulmelk

FSTT, Abdelmalek Essaadi University

Research Article

Keywords: Fractional Laplacian, Space-time fractional equation, inverse source problem, Caputo derivative, unknown terminal time

Posted Date: July 27th, 2026

DOI: https://doi.org/10.21203/rs.3.rs-10412671/v1

License: This work is licensed under a Creative Commons Attribution 4.0 International License.
Read Full License

Additional Declarations: No competing interests reported.

Stable reconstruction of a spatial source term in a time-space fractional diffusion equation using Tikhonov regularization and final-time measurements

Ihya Talibi[a], Abdessamad Oulmelk[b,]

[a] *FST Béni Mellal; Sultan Moulay Slimane University, Morocco*
[b] *Laboratory of mathematics and applications, FSTT, Abdelmalek Essaadi University, Tetouan, Morocco*

Abstract

This paper is devoted to the investigation of an inverse source problem associated with a fractional time-space diffusion equation. The main goal is to recover a space-dependent source term from noisy final-time observations. First, the well-posedness of the corresponding direct problem is established through a rigorous theoretical analysis. Subsequently, the inverse problem, which is inherently ill-posed, is reformulated as an optimization problem. In this framework, we study the existence of minimizers together with the uniqueness and stability properties of the proposed formulation. To overcome the ill-posedness, the Tikhonov regularization technique is employed, and the resulting regularized solution is computed using a gradient descent algorithm. Finally, several numerical reconstruction experiments are presented to illustrate the effectiveness, stability, and accuracy of the proposed approach.

Keywords: Fractional Laplacian, Space-time fractional equation, inverse source problem, Caputo derivative, unknown terminal time

1. Introduction

Fractional diffusion equations have emerged as powerful modeling tools in various scientific and engineering disciplines, precisely because they capture two fundamental features that classical diffusion models ignore: *memory* (via time-fractional derivatives) and *long-range interactions* (via space-fractional Laplacians). These features are essential for describing anomalous diffusion processes, where the mean-square displacement grows nonlinearly with time, as observed in phenomena such as solute transport in heterogeneous porous media, protein movement in cell membranes, and heat conduction in fractal materials. However, in many practical situations, the source term driving such fractional diffusion processes is not directly accessible. Instead, only indirect observationssuch as the final concentration or temperature distribution at a given time $T$are available. The ability to reconstruct an unknown spatial source from such terminal measurements is of paramount importance for applications ranging from pollutant source identification in groundwater hydrology to thermal source recovery in nanostructured materials. This work is precisely motivated by this practical need: given a final-time measurement $y(x,T)$, can we uniquely and stably recover a space-dependent source term $f(x)$ in a time-space fractional diffusion equation, and how can we do this numerically in the presence of noisy data?

Let $\Omega \subset \mathbb{R}^d$ $(d = 1, 2, 3)$ be a bounded open domain, and let $T > 0$ denote the final time. We consider the following time-space fractional diffusion problem:

$$\begin{cases} \partial_t^\alpha y + (-\Delta)^s y + ay &= F \quad \text{in} \quad \Omega \times (0,T], \\ y &= 0 \quad \text{in} \quad \mathbb{R}^d \setminus \Omega \times (0,T], \\ y(\cdot,0) &= y_0 \quad \text{in} \quad \Omega, \end{cases} \tag{1}$$

Email addresses: ihya.talibi@usms.ma (Ihya Talibi), a.oulmelk@uae.ac.ma (Abdessamad Oulmelk)

where $F \in L^2(0,T;L^2(\Omega))$ is the source term, $y_0 \in L^2(\Omega)$ is the initial condition, and $a \in L^\infty(\Omega)$ is a strictly positive potential coefficient depending on the spatial variable.

In this model, ∂_t^α denotes the Djrbashian–Caputo fractional derivative of order $\alpha \in (0,1)$, defined by

$$\partial_t^\alpha y = \frac{1}{\Gamma(1-\alpha)} \int_0^t (t-s)^{-\alpha} y'(s)\, ds, \tag{2}$$

where Γ is the Gamma function given by

$$\Gamma(z) = \int_0^\infty s^{z-1} e^{-s}\, ds. \tag{3}$$

The operator $(-\Delta)^s$, with $0 < s < 1$, represents the fractional Laplacian defined as

$$(-\Delta)^s h(x) := C_{d,s}\, \text{P.V.} \int_{\mathbb{R}^d} \frac{h(x)-h(y)}{|x-y|^{d+2s}}\, dy, \tag{4}$$

where P.V. denotes the Cauchy principal value:

$$\text{P.V.} \int_{\mathbb{R}^d} \frac{h(x)-h(y)}{|x-y|^{d+2s}}\, dy = \lim_{\varepsilon \to 0} \int_{\mathbb{R}^d \setminus B_\varepsilon(x)} \frac{h(x)-h(y)}{|x-y|^{d+2s}}\, dy. \tag{5}$$

Here, $B_\varepsilon(x)$ is the ball centered at x with radius ε, and the normalization constant $C_{d,s}$ is given by

$$C_{d,s} = \frac{4^s}{\pi^{d/2}} \frac{\Gamma\left(\frac{d}{2}+s\right)}{|\Gamma(-s)|}. \tag{6}$$

Fractional partial differential equations have become an important mathematical tool for modeling various complex phenomena involving memory and nonlocal effects. Such models arise in many applications from physics, biology, engineering, and finance. In particular, the classical diffusion equation has been successfully generalized by replacing the standard Laplacian with the fractional Laplacian, which naturally describes long-range interactions and anomalous diffusion processes. This operator is closely related to Lévy processes and random walks with long jumps. This operator can be derived from a probabilistic framework, such as the upper bound of the long jump random walk [1]. Moreover, These models find additional uses in various fields such as geophysics [2], anomalous transport and diffusion, image noising phase-field [3], porous media flow [4], data analysis [5], elasticity [6], and population dynamics [7]. The space-fractional partial derivative for the diffusion equations (SFDE) is well-posed. This fractional model can be utilized to explain abnormal diffusion which corresponds to fractional Brownian motion. In recent years, there has been thorough theoretical and numerical study of the initial boundary value problems associated with the SFDE as direct problems.

In recent studies conducted by [8] and [5], significant attention has been given to exploring the direct and inverse problems associated with time-space fractional parabolic equations. These investigations specifically focus on diverse abstract self-adjoint operators, aiming to deepen our understanding of the behavior and characteristics of such equations. Underline that the fractional derivative $\partial_t^\alpha y$ coincides with the usual first-order derivative $\partial_t y$ when $\alpha \to 1^-$. Thus problem (1) amounts to a classical parabolic problem. The modeling of problem (1) can be encountered, among other things, in the study of abnormally slow diffusion processes. Among the applications which have shown great success we can cite: thermal diffusion in fractional media in Physics [3], the dispersion of ions in column experiments in Engineering [9] and the transport of proteins in membranes in Biology [10]. Hence several authors have been interested in the study of this problem, see for example [5, 11, 12]. The references [5] and [12–14] extensively cover a wide range of inverse source problems and coefficient identification.

In practice, when it comes to measurement data, the choice of observation $\mathcal{Z}(x) = y(x,T), x \in \Omega$, at a finite time T is very known and a classical choice. Based on final observational data, multiple works on inverse source and potential problems are available [15–19]. As for the problem of sub-diffusion, we may refer to the following references [12, 20]. Thus, the uniqueness and stability of the solution of the inverse problem has been studied and demonstrated. Moreover, for the problem of ill-posed sub-diffusion, Lipschitz stability is proved see for example [12].

Indeed, utilizing the observations $y(T)$ at a terminal time T, we investigate the inverse problem of determining the space-dependent source term. Under fitting a prior regularity assumptions on the initial data y_0 and the source F, we will establish the unique recovery of the space-dependent parameter from the terminal observation . The study mainly relies on explicit solution representations in the form of Mittag-Leffler functions. (see, e.g., [12]). As referenced in [21] and other studies [22, 23], the determination of $F = F(x,t)$ becomes highly challenging when it depends on both space and time. It is clear from the literature that much research on source determination mainly focuses on special cases, such as $F = g(t)$ or $F = f(x)$ or their product $F = g(t)f(x)$, given g or f. In this context, there are many works, for example, the authors in [24] used the regularized control optimal approach under two different cost functions to analyse an inverse source problem for a time-fractional diffusion equation, and in [25] they solved an inverse source problem for a subdiffusion model on the basis of the optimal control method. Also in [26] they investigated an inverse time-dependent source problem for a multi-dimensional fractional diffusion equation from boundary Cauchy data. In this paper, we make the assumption that the source term, denoted as F, is solely dependent on space. Specifically, it takes the form $F(x,t) = g(t)f(x)$, where $g \in L^2(0,T)$ is a known function and $f \in L^2(\Omega)$ is an unknown function. As previously stated, our objective is to identify the unknown term based on final data.

The main contribution of this work is both theoretical and numerical. First, we establish the well-posedness of the direct problem and derive explicit representations of the solution involving MittagLeffler functions. Next, the inverse source problem is reformulated as an optimization problem. Since this inverse problem is ill-posed, we employ the classical Tikhonov regularization method to stabilize the reconstruction procedure. We then investigate the existence, uniqueness, and stability of the corresponding minimization problem.

From the numerical point of view, we develop a reconstruction algorithm based on a gradient descent approach. One of the main difficulties in the numerical implementation comes from the approximation of the nonlocal fractional Laplacian operator. Finally, several numerical experiments are presented to illustrate the efficiency, stability, and accuracy of the proposed method.

The remainder of this paper is organized as follows. In Section 2, we introduce the mathematical preliminaries and some useful properties related to fractional operators. Section 3 is devoted to the study of the direct problem and the proof of existence and uniqueness results. In Section 4, we formulate the inverse source problem as an optimization problem and study the associated Tikhonov regularization method. Section 5 presents the numerical reconstruction algorithm together with several numerical examples. Finally, Section 6 concludes the paper with some remarks and perspectives for future work.

2. Preliminaries and uniqueness of the inverse problem

In this section, we introduce the necessary notation and review essential results from fractional calculus. These tools play a crucial role in the analysis of the forward problem (1). Familiarity with these concepts will facilitate the understanding of the inverse problem studied thereafter.

For $s \in (0,1)$, the fractional Sobolev space $K^s(\Omega)$ is defined as

$$K^s(\Omega) = \left\{ h \in L^2(\Omega) : \int_{\mathbb{R}^d} \int_{\mathbb{R}^d} \frac{|h(x) - h(y)|^2}{|x-y|^{d+2s}}\, dx\, dy < \infty \right\}. \tag{7}$$

The space $K^s(\Omega)$ is a Hilbert space equipped with the norm

$$\|h\|_{K^s(\Omega)} = \left(\|h\|^2_{L^2(\Omega)} + |h|^2_{K^s(\Omega)} \right)^{\frac{1}{2}}, \tag{8}$$

where $|h|_{K^s(\Omega)}$ denotes the Aronszajn–Slobodeckij seminorm defined by

$$|h|_{K^s(\Omega)} = \int_{\mathbb{R}^d} \int_{\mathbb{R}^d} \frac{|h(x) - h(y)|^2}{|x-y|^{d+2s}}\, dx\, dy. \tag{9}$$

We also introduce the space $\tilde{K}^s(\Omega)$, which consists of functions belonging to $K^s(\mathbb{R}^d)$ whose support is contained in the closure of Ω:

$$\tilde{K}^s(\Omega) := \left\{ w \in K^s(\mathbb{R}^d) : \mathrm{supp}(w) \subset \overline{\Omega} \right\}. \tag{10}$$

The associated bilinear form on $\tilde{K}^s(\Omega)$ is given by

$$\langle u, h\rangle_s = C_{d,s} \int_{\mathbb{R}^d} \int_{\mathbb{R}^d} \frac{(u(x)-u(y))(h(x)-h(y))}{|x-y|^{d+2s}}\, dx\, dy. \tag{11}$$

The forward and backward Riemann–Liouville integral operators of order $\alpha \in (0,1)$ are defined respectively by

$$\mathcal{I}^{\alpha}_{0+} u(t) := \frac{1}{\Gamma(\alpha)} \int_0^t (t-\tau)^{\alpha-1} u(\tau)\, d\tau, \qquad \mathcal{I}^{\alpha}_{T-} u(t) := \frac{1}{\Gamma(\alpha)} \int_t^T (\tau - t)^{\alpha-1} u(\tau)\, d\tau. \tag{12}$$

The corresponding forward and backward Riemann–Liouville fractional derivatives are given by

$$D^{\alpha}_{0+} u(t) := \frac{1}{\Gamma(1-\alpha)} \frac{d}{dt} \int_0^t (t-\tau)^{-\alpha} u(\tau)\, d\tau, \qquad D^{\alpha}_{T-} u(t) := \frac{1}{\Gamma(1-\alpha)} \left(-\frac{d}{dt}\right) \int_t^T (\tau - t)^{-\alpha} u(\tau)\, d\tau. \tag{13}$$

The following lemma provides an integration-by-parts formula linking the Caputo and Riemann–Liouville fractional derivatives.

Lemma 1 (Fractional integration by parts [27]). *Let u_1, u_2 be absolutely continuous functions on $[0,T]$. Then*

$$\int_0^T u_2(t)\, \partial_t^{\alpha} u_1(t)\, dt = \int_0^T u_1(t)\, D^{\alpha}_{T-} u_2(t)\, dt + \left[u_1(t)\, \mathcal{I}^{1-\alpha}_{T-} u_2(t)\right]_{t=0}^{t=T}. \tag{14}$$

The following theorem establishes the existence and uniqueness of a solution to problem (1).

Theorem 1. *Let $0 < \alpha, s < 1$, $f \in L^2(\Omega)$ and $g \in L^2(0,T)$ with $g(t) > 0$ almost everywhere. Then problem (1) with $F(x,t) = g(t)f(x)$ admits a unique solution*

$$y \in L^2\Big(0,T; \tilde{K}^s(\Omega) \cap H^{s+\zeta}(\Omega)\Big), \qquad \partial_t^{\alpha} y \in L^2(\Omega \times (0,T)), \tag{15}$$

where the regularity parameter $\zeta \in (0, 1/2)$ is defined to ensure the embedding $H^{s+\zeta}(\Omega) \hookrightarrow L^2(\Omega)$ is continuous. In practice, we may take $\zeta = \min\{s, 1/4\}$.. Moreover, there exists a constant $C > 0$ such that

$$\|\partial_t^{\alpha} y\|_{L^2(\Omega\times(0,T))} + \|y\|_{L^2(0,T;H^{s+\zeta}(\Omega))} \le C \|f\|_{L^2(\Omega)}. \tag{16}$$

Proof The proof follows the arguments developed for time-space fractional problems in [28].

Before stating the weak formulation, we introduce the following function spaces:

$$\mathcal{Y} := L^2(0,T; \tilde{K}^s(\Omega)), \tag{17}$$

$$\mathcal{Y}^{\alpha,s}\big(0,T; L^2(\Omega)\big) := L^2\Big(0,T; \tilde{K}^s(\Omega) \cap K^{s+\zeta}(\Omega)\Big). \tag{18}$$

Definition 2.1 (Weak solution). *A function $y \in \mathcal{Y}^{\alpha,s}(0,T; L^2(\Omega))$ is called a weak solution of problem (1) if it satisfies the variational formulation*

$$\langle \partial_t^{\alpha} y(\cdot,t), w\rangle_{-s,s} + \mathcal{A}(y(\cdot,t), w) = \langle fg, w\rangle, \qquad \forall w \in \tilde{K}^s(\Omega), \tag{19}$$

where the bilinear form $\mathcal{A}(\cdot,\cdot)$ is defined by

$$\mathcal{A}(w,v) = \frac{C_{d,s}}{2} \int_{\mathbb{R}^d} \int_{\mathbb{R}^d} \frac{(w(x)-w(y))(v(x)-v(y))}{|x-y|^{d+2s}}\, dx\, dy. \tag{20}$$

We now prove that the space-dependent source term f is uniquely determined by the final-time measurement $y(\cdot, T)$.

Theorem 2 (Uniqueness). *Let $g \in C([0,T])$ be a nonnegative, nonzero function. For $l = 1, 2$, let y_l be the solutions of*

$$\begin{cases} \partial_t^\alpha y_l + (-\Delta)^s y_l + a y_l &= f_l(x)\, g(t) \quad in \quad \Omega \times (0,T], \\ y_l &= 0 \quad in \quad \mathbb{R}^d \setminus \Omega \times (0,T], \\ y_l(\cdot,0) &= 0 \quad in \quad \Omega, \end{cases} \tag{21}$$

with $f_l \in L^2(\Omega)$. Assume that the final-time observations coincide, i.e.,

$$y_1(\cdot,T) = y_2(\cdot,T) \quad in\ \Omega. \tag{22}$$

Then $f_1 = f_2$ in $L^2(\Omega)$.

Proof Consider the difference $y_{2,1} := y_2 - y_1$, which satisfies

$$\begin{cases} \partial_t^\alpha y_{2,1} + (-\Delta)^s y_{2,1} + a y_{2,1} &= (f_2 - f_1)(x)\, g(t) \quad \text{in} \quad \Omega \times (0,T], \\ y_{2,1} &= 0 \quad \text{in} \quad \mathbb{R}^d \setminus \Omega \times (0,T], \\ y_{2,1}(\cdot,0) &= 0 \quad \text{in} \quad \Omega. \end{cases} \tag{23}$$

From (22), we have

$$y_{2,1}(\cdot,T) = 0 \quad \text{in } \Omega. \tag{24}$$

The solution $y_{2,1} \in \mathcal{Y}^{\alpha,s}(0,T;L^2(\Omega))$ admits the spectral representation

$$y_{2,1}^k(t) = \mathcal{F}^k(t)\,(f_2 - f_1)^k\, g(t), \tag{25}$$

where

$$\mathcal{F}^k w = \int_0^t (t-r)^{\alpha-1} E_{\alpha,\alpha}\big(-\lambda^k (t-r)^\alpha\big)\, w(r)\, dr, \tag{26}$$

and $E_{\alpha,\alpha}(z) = \sum_{k=0}^{\infty} \frac{z^k}{\Gamma(\alpha k + \alpha)}$ is the two-parameter Mittag–Leffler function. The quantities λ^k denote the eigenvalues of the fractional Laplacian.

Taking the inner product with $f_{2,1} := f_2 - f_1$ yields

$$\langle y_{2,1}(\cdot,t), f_{2,1}\rangle = \left\langle f_{2,1} \int_0^t (t-r)^{\alpha-1} E_{\alpha,\alpha}\big(-\lambda^k (t-r)^\alpha\big)\, g(r)\, dr,\ f_{2,1} \right\rangle. \tag{27}$$

Evaluating at $t = T$ and using (24), we obtain

$$0 = \langle y_{2,1}(\cdot,T), f_{2,1}\rangle = \left\langle f_{2,1} \int_0^T (T-r)^{\alpha-1} E_{\alpha,\alpha}\big(-\lambda^k (T-r)^\alpha\big)\, g(r)\, dr,\ f_{2,1} \right\rangle. \tag{28}$$

By Lemma 4.1 in [8], the kernel

$$\int_0^T (T-r)^{\alpha-1} E_{\alpha,\alpha}\big(-\lambda^k (T-r)^\alpha\big)\, g(r)\, dr > 0, \tag{29}$$

for each k, since g is nonnegative and not identically zero. Therefore we conclude $f_{2,1} = 0$ in $L^2(\Omega)$, i.e., $f_1 = f_2$. This completes the proof of uniqueness for the inverse source problem.

3. Stability analysis and regularization

In this section, we focus on the second objective of this study: developing an effective numerical method for reconstructing the spatial component of the source term in the time-space fractional diffusion equation (1). The reconstruction relies on the final-time observations $\mathcal{Z}(x) = y(x,T)$ for $x \in \Omega$.

The inverse source problem is reformulated as a least-squares minimization problem, a common approach in the literature. For a given $f \in L^2(\Omega)$ (serving as an initial guess), we denote by y_f the solution of the forward problem:

$$\begin{cases} \partial_t^\alpha y(f) + (-\Delta)^s y(f) + a\, y(f) &= F \quad \text{in} \quad \Omega \times (0,T], \\ y(f) &= 0 \quad \text{in} \quad \mathbb{R}^d \setminus \Omega \times (0,T], \\ y(f)(\cdot,0) &= y_0 \quad \text{in} \quad \Omega. \end{cases} \tag{30}$$

Suppose we are given noisy observation data $\mathcal{Z}^\delta \in L^2(\Omega)$ satisfying

$$\left\| \mathcal{Z}^\delta - y(f)(\cdot,T) \right\|_{L^2(\Omega)}^2 \leq \varepsilon, \tag{31}$$

where $f \in L^2(\Omega)$ is the true source term and $\varepsilon > 0$ represents the noise level. To address the ill-posedness of problem (1), we employ Tikhonov regularization. Specifically, we consider the following regularized cost functional:

$$\mathcal{L}_\eta(f) = \left\| y(\cdot,T) - \mathcal{Z}^\delta(\cdot) \right\|_{L^2(\Omega)}^2 + \eta \|f\|_{L^2(\Omega)}^2, \tag{32}$$

where $\eta > 0$ is the Tikhonov regularization parameter. The unknown source term is then obtained as the solution of the minimization problem:

$$\underset{f \in L^2(\Omega)}{\text{Minimize}}\, \mathcal{L}_\eta(f). \tag{33}$$

Proposition 1. *The functional $\mathcal{L}_\eta$ defined in (32) admits a minimizer on $L^2(\Omega)$. Furthermore, there exists an element $f^* \in L^2(\Omega)$ and a sequence $\{f^n\}_{n\geq 1} \subset L^2(\Omega)$ such that*

$$f^n \rightharpoonup f^* \quad \text{in } L^2(\Omega) \text{ as } n \to \infty. \tag{34}$$

Proof Since $\mathcal{L}_\eta$ is nonnegative, there exists a minimizing sequence $\{f^n\}_{n\geq 1}$ such that

$$\lim_{n\to\infty} \mathcal{L}_\eta(f^n) = \inf_{f \in L^2(\Omega)} \mathcal{L}_\eta(f). \tag{35}$$

Consequently, for every $n \in \mathbb{N}$, we have

$$0 \leq \mathcal{L}_\eta(f^n) \leq \inf_{f \in L^2(\Omega)} \mathcal{L}_\eta(f) + \frac{1}{n} \leq \mathcal{L}_\eta(f) + \frac{1}{n}. \tag{36}$$

Substituting the definition of $\mathcal{L}_\eta$, we obtain

$$0 \leq \mathcal{L}_\eta(f^n) \leq \left\| y_{f^n}(\cdot,T) - \mathcal{Z}^\varepsilon(\cdot) \right\|_{L^2(\Omega)}^2 + \frac{1}{n} \leq C, \tag{37}$$

which implies that the sequence $\{f^n\}$ is bounded in $L^2(\Omega)$:

$$\|f^n\|_{L^2(\Omega)} \leq C, \quad \forall n \in \mathbb{N}. \tag{38}$$

By the Banach–Alaoglu theorem, there exists a subsequence (still denoted $\{f^n\}$) and an element $f^* \in L^2(\Omega)$ such that $f^n \rightharpoonup f^*$ in $L^2(\Omega)$ as $n \to \infty$.

Theorem 3. *For any $\eta > 0$, the minimization problem (33) has at least one solution.*

Proof We show that the weak limit f^* obtained in Proposition 1 is indeed a minimizer. For each n, let $y(f^n)$ denote the solution of (1) corresponding to f^n. By Theorem 1, the sequence $\{y(f^n)\}$ is uniformly bounded in $\mathcal{Y}^{\alpha,s}(0,T;L^2(\Omega))$. Hence, there exists a subsequence (still denoted $\{f^n\}$) and a limit $y^* \in \mathcal{Y}^{\alpha,s}(0,T;L^2(\Omega))$ such that

$$y(f^n) \rightharpoonup y^* \quad \text{in } \mathcal{Y}^{\alpha,s}(0,T;L^2(\Omega)) \text{ as } n \to \infty. \tag{39}$$

Moreover, by the compactness properties of fractional operators, we have

$$\partial_t^\alpha y(f^n) \rightharpoonup \partial_t^\alpha y^* \quad \text{and} \quad (-\Delta)^s y(f^n) \rightharpoonup (-\Delta)^s y^* \quad \text{as } n \to \infty. \tag{40}$$

The weak formulation for $y(f^n)$ reads

$$\int_\Omega \int_0^T \big(\partial_t^\alpha y(f^n) + (-\Delta)^s y(f^n)\big)\psi \, dx\, dt + \int_\Omega \int_0^T a\, y(f^n)\psi \, dx\, dt$$
$$= \int_0^T \int_\Omega f^n g\psi \, dx\, dt, \qquad \forall \psi \in L^2\big((0,T); \tilde{K}^s(\Omega)\big).$$

Passing to the limit $n \to \infty$ yields

$$\int_\Omega \int_0^T \big(\partial_t^\alpha y^* + (-\Delta)^s y^*\big)\psi \, dx\, dt + \int_0^T \int_\Omega a\, y^*\psi \, dx\, dt$$
$$= \int_0^T \int_\Omega f^* g\psi \, dx\, dt, \qquad \forall \psi \in L^2\big((0,T); \tilde{K}^s(\Omega)\big).$$

To verify that $y^* = y(f^*)$, it suffices to check the initial condition. Using the integration-by-parts formula (14) with $\mathcal{I}_{T-}^{1-\alpha}\psi(T) = 0$, we have

$$\int_\Omega \int_0^T \partial_t^\alpha y(f^n)\psi \, dx\, dt = -\int_\Omega \int_0^T y(f^n) \frac{d}{dt}\mathcal{I}_{T-}^{1-\alpha}\psi \, dx\, dt. \tag{41}$$

Taking the limit $n \to \infty$ gives

$$\int_\Omega \int_0^T \partial_t^\alpha y^*\psi \, dx\, dt = -\int_\Omega \int_0^T y^* \frac{d}{dt}\mathcal{I}_{T-}^{1-\alpha}\psi \, dx\, dt. \tag{42}$$

On the other hand, applying the integration-by-parts formula directly to y^* yields

$$\int_\Omega \int_0^T \partial_t^\alpha y^*\psi \, dx\, dt = -\int_\Omega y^*(\cdot,0)\mathcal{I}_{T-}^{1-\alpha}\psi(\cdot,0)\, dx - \int_\Omega \int_0^T y^* \frac{d}{dt}\mathcal{I}_{T-}^{1-\alpha}\psi \, dx\, dt. \tag{43}$$

Comparing the last two equalities, we conclude that $y^*(\cdot,0) = 0$ in Ω, which coincides with the initial condition for $y(f^*)$. Hence $y^* = y(f^*)$.

Finally, by the weak lower semicontinuity of the L^2-norm, we obtain

$$\begin{aligned}\mathcal{L}_\eta(f^*) &= \|y(f^*)(\cdot,T) - \mathcal{Z}^\varepsilon\|_{L^2(\Omega)}^2 + \eta\|f^*\|_{L^2(\Omega)}^2 \\ &\le \liminf_{n\to\infty} \|y(f^n)(\cdot,T) - \mathcal{Z}^\varepsilon\|_{L^2(\Omega)}^2 + \eta \liminf_{n\to\infty} \|f^n\|_{L^2(\Omega)}^2 \\ &\le \liminf_{n\to\infty} \mathcal{L}_\eta(f^n) = \inf_{f\in L^2(\Omega)} \mathcal{L}_\eta(f).\end{aligned}$$

Thus f^* is a minimizer. Uniqueness follows from the strict convexity of $\mathcal{L}_\eta$.

We now establish that the minimization problem (33) is stable with respect to perturbations in the final-time observation data.

Theorem 4. *Let $\{\mathcal{Z}_n^\varepsilon\}_{n\ge1} \subset L^2(\Omega)$ be a sequence such that*

$$\mathcal{Z}_n^\varepsilon \to \mathcal{Z}^\varepsilon \quad \text{in } L^2(\Omega) \text{ as } n \to \infty. \tag{44}$$

For each n, let f^n be a minimizer of the perturbed functional

$$\mathcal{L}_\eta^n(f) = \|y(f)(\cdot,T) - \mathcal{Z}_n^\varepsilon(\cdot)\|_{L^2(\Omega)}^2 + \eta\|f\|_{L^2(\Omega)}^2. \tag{45}$$

Then $\{f^n\}$ converges strongly in $L^2(\Omega)$ to the unique minimizer f^* of the original problem (33).

Proof The sequence $\{f^n\}$ is bounded in $L^2(\Omega)$ (by an argument similar to Proposition 1). Hence there exists a subsequence (still denoted $\{f^n\}$) and an element $f^* \in L^2(\Omega)$ such that $f^n \rightharpoonup f^*$ in $L^2(\Omega)$. Following the same reasoning as in Theorem 3, we obtain

$$y(f^n) \rightharpoonup y(f^*) \quad \text{in } \mathcal{Y}^{\alpha,s}(0,T;L^2(\Omega)). \tag{46}$$

By the weak lower semicontinuity of the norm,

$$\|y(f) - \mathcal{Z}^\varepsilon\|^2_{L^2(\Omega)} \le \liminf_{n\to\infty} \|y(f^n) - \mathcal{Z}^\varepsilon_n\|^2_{L^2(\Omega)}. \tag{47}$$

For any $f \in L^2(\Omega)$, we have

$$\begin{aligned}
\mathcal{L}_\eta(f^*) &\le \liminf_{n\to\infty} \|y(f^n) - \mathcal{Z}^\varepsilon_n\|^2_{L^2(\Omega)} + \eta \liminf_{n\to\infty} \|f^n\|^2_{L^2(\Omega)} \\
&\le \liminf_{n\to\infty} \left(\|y(f^n) - \mathcal{Z}^\varepsilon_n\|^2_{L^2(\Omega)} + \eta \|f^n\|^2_{L^2(\Omega)} \right) \\
&\le \|y(f) - \mathcal{Z}^\varepsilon\|^2_{L^2(\Omega)} + \eta \|f\|^2_{L^2(\Omega)} = \mathcal{L}_\eta(f).
\end{aligned}$$

Consequently, f^* is a minimizer of $\mathcal{L}_\eta$.

To prove strong convergence, assume for contradiction that $\{f^n\}$ does not converge strongly to f^*. Then, by the weak convergence $f^n \rightharpoonup f^*$ and the weak lower semicontinuity of the norm, we have

$$\|f^*\|_{L^2(\Omega)} \le \liminf_{n\to\infty} \|f^n\|_{L^2(\Omega)} < \limsup_{n\to\infty} \|f^n\|_{L^2(\Omega)}. \tag{48}$$

Choose a subsequence $\{f^k\}$ such that $\limsup_{n\to\infty} \|f^n\|_{L^2(\Omega)} = \lim_{k\to\infty} \|f^k\|_{L^2(\Omega)}$. From the optimality properties, we derive

$$\begin{aligned}
\|y(f^*)(\cdot,T) - \mathcal{Z}^\varepsilon\|^2_{L^2(\Omega)} &= \liminf_{k\to\infty} \|y(f^k) - \mathcal{Z}^\varepsilon_k\|^2_{L^2(\Omega)} \\
&\quad + \eta \left(\left(\limsup_{k\to\infty} \|f^k\|_{L^2(\Omega)} \right)^2 - \|f^*\|^2_{L^2(\Omega)} \right) \\
&> \liminf_{k\to\infty} \|y(f^k) - \mathcal{Z}^\varepsilon_k\|^2_{L^2(\Omega)},
\end{aligned}$$

which contradicts (47). Hence $\|f^n\|_{L^2(\Omega)} \to \|f^*\|_{L^2(\Omega)}$, and together with weak convergence, this implies strong convergence $f^n \to f^*$ in $L^2(\Omega)$.

4. Identification approach

In this section, we develop a numerical method for solving the minimization problem (33). To tackle this variational problem, we employ a gradient descent approach. The main task is to compute the gradient of the Tikhonov functional (32). This is achieved by introducing an adjoint problem and a sensitivity problem.

We consider the following adjoint problem:

$$\begin{cases}
D^\alpha_{T-} p + (-\Delta)^s p + ap &= 0 \quad \text{in} \quad \Omega \times (0,T], \\
p &= 0 \quad \text{in} \quad (\mathbb{R}^d \setminus \Omega) \times (0,T], \\
\mathcal{I}^{1-\alpha}_{T-} p(\cdot,T) &= y(\cdot,T) - \mathcal{Z}^\varepsilon \quad \text{in} \quad \Omega.
\end{cases} \tag{49}$$

The following theorem establishes the Fréchet differentiability of $\mathcal{L}_\eta$ and provides an explicit formula for its gradient.

Theorem 5. *The cost functional $\mathcal{L}_\eta$ is Fréchet differentiable, and its gradient is given by*

$$\nabla \mathcal{L}_\eta(f) = 2 \left(\int_\Omega y(\cdot,T)\, p \, dx + \eta f \right), \tag{50}$$

where p is the solution of the adjoint problem (49).

Proof Let $\delta f \in L^2(\Omega)$ be a variation of f. The corresponding variation of the cost functional is

$$\begin{aligned}
\mathcal{L}_\eta(f+\delta f) - \mathcal{L}_\eta(f) &= \big\| y(f+\delta f)(\cdot,T) - \mathcal{Z} \big\|^2_{L^2(\Omega)} - \big\| y(f)(\cdot,T) - \mathcal{Z} \big\|^2_{L^2(\Omega)} \\
&\quad + \eta \big\| f + \delta f \big\|^2_{L^2(\Omega)} - \eta \big\| f \big\|^2_{L^2(\Omega)} + o\big(\|\delta f\|_{L^2(\Omega)} \big)
\end{aligned}$$

$$= 2\int_\Omega \big(y(f)(\cdot,T) - \mathcal{Z}\big)\,\delta y(f)(\cdot,T)\,dx + 2\int_\Omega f\,\delta f\,dx + o\big(\|\delta f\|_{L^2(\Omega)}\big). \tag{51}$$

Here, $\delta y(\delta f) := y'(f)\delta f$ is the solution of the sensitivity problem:

$$\begin{cases} \partial_t^\alpha \delta y(\delta f) + (-\Delta)^s \delta y(\delta f) + a\,\delta y(\delta f) &= g\,\delta f \quad \text{in} \quad \Omega\times(0,T], \\ \delta y(\delta f) &= 0 \quad \text{in} \quad (\mathbb{R}^d\setminus\Omega)\times(0,T], \\ \delta y(\delta f)(\cdot,0) &= 0 \quad \text{in} \quad \Omega. \end{cases} \tag{52}$$

Multiplying the sensitivity equation by $p(x,t)$ and integrating over $\Omega\times(0,T)$, we obtain

$$\int_\Omega \delta y(x,T)\,\mathcal{I}_{T-}^{1-\alpha} p(x,T)\,dx + \int_\Omega\int_0^T \delta y(x,t)\,D_{T-}^{\alpha} p(x,t)\,dx\,dt + \int_0^T \mathcal{A}(\delta y,p)\,dt + \int_\Omega\int_0^T a\,\delta y\,p\,dx\,dt = \int_0^T\int_\Omega g\,\delta f\,p\,dx\,dt. \tag{53}$$

Using the adjoint problem (49) and the fact that δy vanishes at $t=0$, we deduce

$$\int_\Omega \big(y(\cdot,T) - \mathcal{Z}^\varepsilon\big)\delta y(\cdot,T)\,dx = \int_\Omega\int_0^T \delta f(x)\,g(t)\,p(x,t)\,dx\,dt. \tag{54}$$

Substituting (54) into (51) yields

$$\mathcal{L}_\eta(f+\delta f) - \mathcal{L}_\eta(f) = 2\int_\Omega\int_0^T \delta f(x)\,g(t)\,p(x,t)\,dx\,dt + 2\int_\Omega f(x)\,\delta f(x)\,dx + o\big(\|\delta f\|_{L^2(\Omega)}\big). \tag{55}$$

Hence, the Fréchet derivative of $\mathcal{L}_\eta$ at f in the direction δf is given by

$$\langle \nabla\mathcal{L}_\eta(f), \delta f\rangle_{L^2(\Omega)} = 2\int_\Omega \left(\int_0^T g(t)\,p(x,t)\,dt + \eta f(x)\right)\delta f(x)\,dx. \tag{56}$$

Therefore,

$$\nabla\mathcal{L}_\eta(f) = 2\left(\int_0^T g(t)\,p(\cdot,t)\,dt + \eta f\right). \tag{57}$$

Noting that p depends on y through the final-time condition, the expression in (50) follows (see Remark 1 below for a simplified formulation).

Remark 1. *In practice, the term* $\int_0^T g(t)p(\cdot,t)dt$ *is often approximated or simplified. Under appropriate regularity conditions, one can show that*

$$\int_0^T g(t)p(x,t)dt = \int_\Omega y(\cdot,T)\,p(\cdot,T)\,dx, \tag{58}$$

which leads to the compact form (50).

We now apply the conjugate gradient method to find the minimizer of (33). Let f^k denote the approximation at the k-th iteration. The update is given by

$$f^{k+1} = f^k + \xi_k d_k, \tag{59}$$

where the descent direction d_k is defined as

$$d_k = \begin{cases} -\nabla\mathcal{L}_\eta(f^k) & \text{if } k=0, \\ -\nabla\mathcal{L}_\eta(f^k) + \beta_k d_{k-1} & \text{if } k>0, \end{cases} \tag{60}$$

with the Polak–Ribiére (or Fletcher–Reeves) parameter

$$\beta_k = \frac{\left\|\nabla \mathcal{L}_\eta(f^k)\right\|^2_{L^2(\Omega)}}{\left\|\nabla \mathcal{L}_\eta(f^{k-1})\right\|^2_{L^2(\Omega)}}. \tag{61}$$

The step size ξ_k is determined by a line search:

$$\xi_k = \arg\min_{\xi \geq 0} \mathcal{L}_\eta(f^k + \xi d_k). \tag{62}$$

To compute ξ_k explicitly, we introduce the linear operator $A : L^2(\Omega) \to L^2((0,T); \tilde{K}^s(\Omega))$ defined by $Af = y(f)$. Then,

$$\begin{aligned} \mathcal{L}_\eta(f^k + \xi d_k) &= \left\|A(f^k + \xi d_k)(\cdot, T) - \mathcal{Z}\right\|^2_{L^2(\Omega)} + \eta \left\|f^k + \xi d_k\right\|^2_{L^2(\Omega)} \\ &= \left\|Af^k + \xi A d_k - \mathcal{Z}\right\|^2_{L^2(\Omega)} + \eta \left\|f^k + \xi d_k\right\|^2_{L^2(\Omega)}. \end{aligned} \tag{63}$$

Differentiating with respect to ξ and setting the derivative to zero gives

$$\frac{\partial}{\partial \xi} \mathcal{L}_\eta(f^k + \xi d_k) = 2\xi \|Ad_k\|^2_{L^2(\Omega)} + 2\langle Ad_k, Af^k - \mathcal{Z}\rangle + 2\eta\xi \|d_k\|^2_{L^2(\Omega)} + 2\eta \langle d_k, f^k\rangle = 0. \tag{64}$$

Solving for ξ_k, we obtain

$$\xi_k = -\frac{\langle Ad_k, Af^k - \mathcal{Z}\rangle + \eta \langle d_k, f^k\rangle}{\|Ad_k\|^2_{L^2(\Omega)} + \eta \|d_k\|^2_{L^2(\Omega)}}. \tag{65}$$

Using the relation $\langle Ad_k, Af^k - \mathcal{Z}\rangle = \langle d_k, \nabla \mathcal{L}_\eta(f^k)\rangle/2 - \eta \langle d_k, f^k\rangle$ (which follows from the gradient expression), we can simplify:

$$\xi_k = -\frac{\langle d_k, \nabla \mathcal{L}_\eta(f^k)\rangle_{L^2(\Omega)}}{\|Ad_k\|^2_{L^2(\Omega)} + \eta \|d_k\|^2_{L^2(\Omega)}}. \tag{66}$$

Since the conjugate gradient method ensures $\langle d_k, \nabla \mathcal{L}_\eta(f^k)\rangle = -\|\nabla \mathcal{L}_\eta(f^k)\|^2_{L^2(\Omega)}$ (for exact line search), we finally have

$$\xi_k = \frac{\left\|\nabla \mathcal{L}_\eta(f^k)\right\|^2_{L^2(\Omega)}}{\|Ad_k\|^2_{L^2(\Omega)} + \eta \|d_k\|^2_{L^2(\Omega)}}. \tag{67}$$

Equivalently, in terms of the solution $y_k = Ad_k$,

$$\xi_k = -\frac{\displaystyle\int_\Omega \big(y(f^k)(\cdot, T) - \mathcal{Z}\big) y_k(\cdot, T)\, dx + \eta \int_\Omega f^k d_k\, dx}{\displaystyle\int_\Omega y_k^2(\cdot, T)\, dx + \eta \int_\Omega d_k^2\, dx}. \tag{68}$$

The complete procedure is summarized in Algorithm 1.

Algorithm 1 Conjugate Gradient Algorithm for Minimization Problem (33)

1. Initialize: Set $k = 0$ and choose an initial guess $f^0 \in L^2(\Omega)$ (typically $f^0 = 0$).
2. Compute gradient at f^0:
   (a) Solve forward problem (1) with source $F = g(t)f^0(x)$ and zero initial condition to obtain $y^0 = y(f^0)$.
   (b) Solve adjoint problem (49) with terminal condition $\mathcal{I}_{T-}^{1-\alpha} p(\cdot, T) = y^0(\cdot, T) - \mathcal{Z}^\delta$ to obtain adjoint state p^0.
   (c) Compute gradient: $\nabla \mathcal{L}_\eta(f^0) = 2(\int_0^T g(t)p^0(\cdot, t)dt + \eta f^0)$.
3. Set descent direction: $r_0 = -\nabla \mathcal{L}_\eta(f^0)$ and $d_0 = r_0$.
4. Compute step size:
$$\xi_0 = \frac{\|r_0\|^2_{L^2(\Omega)}}{\|Ad_0\|^2_{L^2(\Omega)} + \eta\|d_0\|^2_{L^2(\Omega)}},$$
   where Ad_0 is obtained by solving the forward problem with $F = g(t)d_0(x)$.
5. Update: $f^1 = f^0 + \xi_0 d_0$.
6. For $k = 1, 2, 3, \ldots$ (until convergence):
   (a) Compute residual: $r_k = -\nabla \mathcal{L}_\eta(f^k)$ (requires solving forward and adjoint problems).
   (b) Compute Polak-Ribiere parameter: $\beta_k = \dfrac{\|r_k\|^2_{L^2(\Omega)}}{\|r_{k-1}\|^2_{L^2(\Omega)}}$.
   (c) Update descent direction: $d_k = r_k + \beta_k d_{k-1}$.
   (d) Compute step size: $\xi_k = \dfrac{\|r_k\|^2_{L^2(\Omega)}}{\|Ad_k\|^2_{L^2(\Omega)} + \eta\|d_k\|^2_{L^2(\Omega)}}$.
   (e) Update solution: $f^{k+1} = f^k + \xi_k d_k$.
7. Stopping criterion: Iterate until $\|\nabla \mathcal{L}_\eta(f^k)\|_{L^2(\Omega)} \leq$ tol or maximum iterations reached.

Remark 2. *In practice, the forward and adjoint problems are discretized using a finite difference or finite element method. The operator Ad_k is evaluated by solving the forward problem (1) with source term $g(t)d_k(x)$ and zero initial condition. The gradient $\nabla \mathcal{L}_\eta(f^k)$ is then computed using the adjoint state p obtained from (49).*

5. Numerical Experiments

In this section, we present the numerical results of four examples in one-dimensional case to show the effectiveness of the proposed iterative algorithm. In our computational procedure, the domain Ω is taken to be the interval $(0, 1)$ and the final time $T = 1$. The forward and adjoint problems are all discretized using the finite difference method developed in [29, 30], with mesh size $\Delta x = 1/75$ and the backward Euler time-stepping on a uniform mesh with time step $\Delta t = 1/51$. By setting the unknown source term f and selecting the second member function g, the initial condition y_0 and the potential parameter a, we construct the synthetic measurement data $\mathcal{Z}$.

Noisy observation data is generated by adding a random perturbation according to

$$\mathcal{Z}^\delta = \mathcal{Z} + \varepsilon \cdot \mathcal{Z} \cdot (2\text{rand}(N) - 1), \tag{69}$$

where rand(N) generates N independent uniformly distributed random variables in $[0, 1]$, and ε represents the relative noise level (expressed as a percentage: 0.1%, 5%, or 10%).

We compute the error represented below to show the accuracy of the numerical solution of the suggested methods. The relative error is defined as

$$\text{Err}(f_m) = \frac{\|f_m - f_{\text{exact}}\|_{L^2(\Omega)}}{\|f_{\text{exact}}\|_{L^2(\Omega)}}, \tag{70}$$

where f_m is the reconstructed source term at iteration m and f_{exact} is the true source term.

The application also needs a stopping condition. In our numerical studies, it was challenging to identify criteria that are applicable to test data that is both synthetic and measured. Since the change in the reconstruction obtained from each iteration step in our case was no longer discernible, the iterative process was interactively monitored and stopped. Then is utilized the calculated relative error presented by

$$Err(f_{m+1}) = \frac{e_m}{\|f_m\|_2}. \tag{71}$$

.

For all numerical experiments, we set the potential parameter $a(x) = x^2 + 1$, the initial condition $y_0(x) = \sin(\pi x)$, and the time-dependent weight $g(t) = \sin(\pi t)$. The specific source terms $f(x)$ and the weight function $g(t)$ are chosen individually for each example as detailed below. The regularization parameter is $\eta = 10^{-6}$, the time-fractional order is $\alpha = 0.5$, and the space-fractional order is $s = 0.3$.

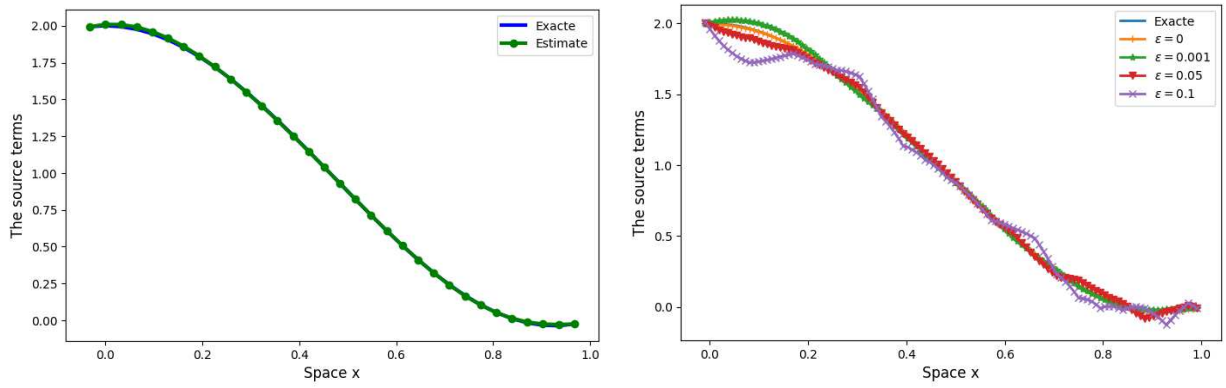
Remark 3. *Finding an appropriate regularization parameter η is challenging in practice. In this work, η was selected via trial-and-error to minimize the reconstruction error on a test set. A systematic parameter selection strategy (e.g., L-curve method, generalized cross-validation) would be a valuable extension.*

We now present four tests in the one-dimensional case to showcase the effectiveness of the suggested methods. The estimation results of the source term f are provided for these examples, which can be categorized into two types: regular examples (Examples 5.1 and 5.2) and complex examples (Examples 5.3 and 5.4).

Example 5.1. *In this experiment, our algorithm is employed to reconstruct an unidentified source term described as follows:*

$$f(x) = x^2(x-1)^2 + \cos(\pi x) + 1.$$

We use $g(t) = \sin(\pi t)$ and solve the forward problem to generate synthetic noisy measurements $\mathcal{Z}^\delta(x) = y(x,T)$ at time $T = 1$. The reconstruction results without noise and with varying noise levels are shown in Figure 1.



(a) Reconstruction without noise

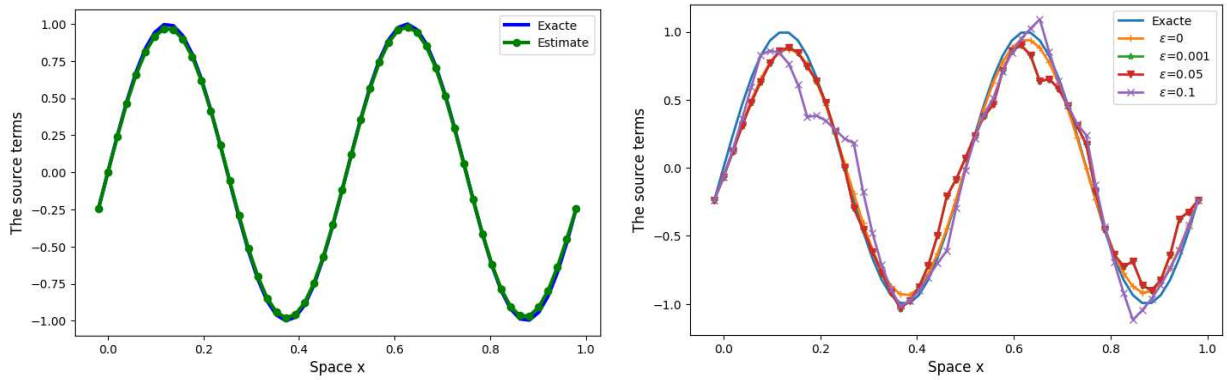
(b) Reconstruction with different noises

Figure 1: The reconstruction of Examples 5.1 with $\alpha = 0.5$ and $s = 0.3$.

Example 5.2. *In the second example, we aim to identify an other example of smooth space-dependent source term*

$$f(x) = \sin(4\pi x),$$

with weight function $g(t) = e^{-t}$. The numerical results without and with various noise levels are illustrated in Figure 2.



(a) Reconstruction without noise

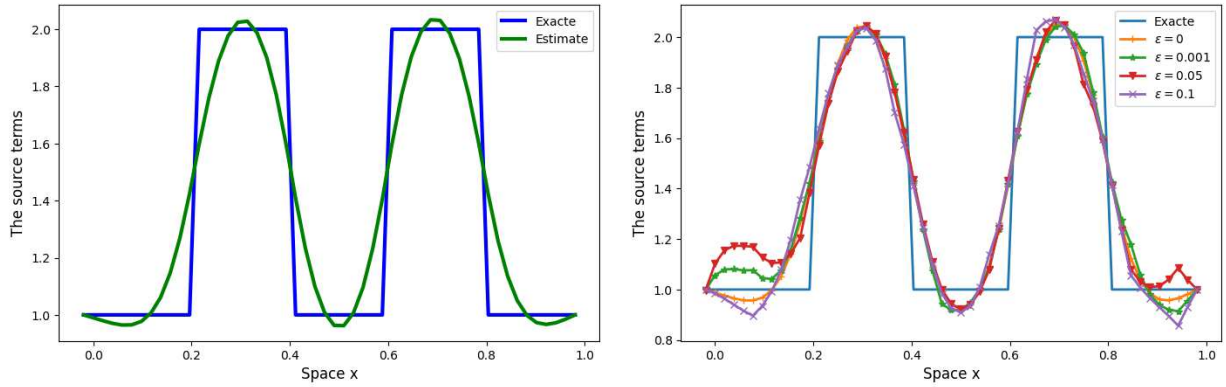
(b) Reconstruction with different noises

Figure 2: The reconstruction of Examples 5.2 with $\alpha = 0.5$ and $s = 0.3$.

Example 5.3. *In this example, we evaluate the algorithm's performance on a piecewise constant (nonsmooth) source term:*

$$f(x) = \begin{cases} 1, & x \in [0, 0.2) \cup [0.4, 0.6) \cup (0.8, 1] \\ 2, & x \in [0.2, 0.4) \cup [0.6, 0.8] \end{cases}$$

with $g(t) = \sin(\pi t)$. *The results demonstrate the method's ability to handle discontinuous sources, though with some smoothing artifacts near jump discontinuities (see Figure 3).*



(a) Reconstruction without noise

(b) Reconstruction with different noises

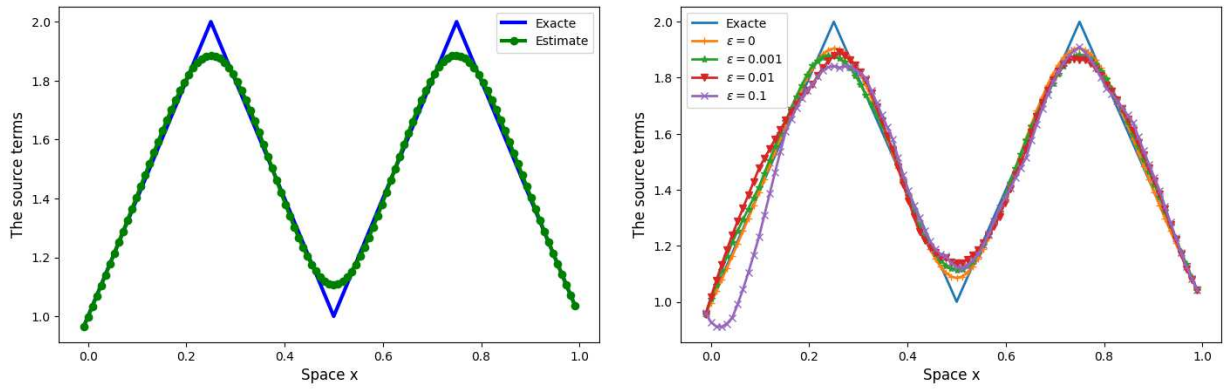
Figure 3: The reconstruction of Examples 5.3 with $\alpha = 0.5$ and $s = 0.3$.

Figure 3 illustrates the numerical results for the given function under different conditions, including without noise and with various noise levels.

Example 5.4. *In the final example, we test the algorithm on a piecewise linear (sawtooth) function:*

$$f(x) = \begin{cases} 4x + 1, & 0 \le x \le 0.25 \\ -4x + 3, & 0.25 \le x \le 0.5 \\ 4x - 1, & 0.5 \le x \le 0.75 \\ -4x + 5, & 0.75 \le x \le 1 \end{cases}$$

with $g(t) = e^{-t}$. *The numerical results in Figure 4 show the reconstruction behavior for this piecewise-linear source with and without noise.*



(a) Reconstruction without noise

(b) Reconstruction with different noises

Figure 4: The reconstruction of Examples 5.4 with $\alpha = 0.5$ and $s = 0.3$.

Figures 4 represent the comparison between the exact source term f and the reconstructed ones.

An important observation to highlight is that the results obtained for the regular cases (Figures 1 and 2) exhibit a close match with the actual source. This indicates that the estimation method performs well in capturing the characteristics of regular sources and accurately reconstructing their values.

However, when dealing with complex sources, the method faces challenges in accurately reconstructing the source singularities. Figures 3 and 4 provides a visual representation of this limitation. It shows that the estimation results for complex sources deviate from the actual source, particularly in capturing the singularities inherent in these sources.

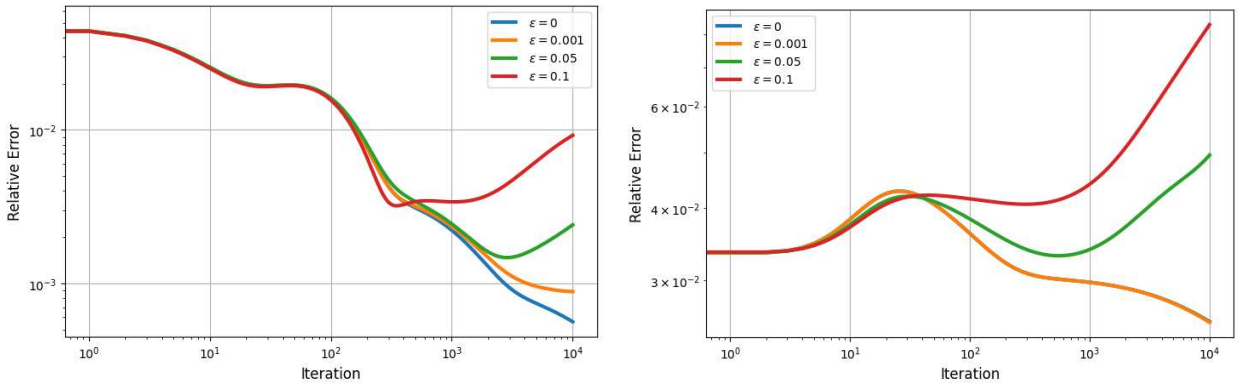
In the conducted numerical tests, we examined the results obtained for different noise levels, specifically at 0.1%, 5%, and 10%. Figures 1(b) and 2(b) showcases the numerical outputs for the regular examples under varying noise levels, while Figures 3(b) and 4(b) displays the numerical outputs for the singular examples with different noise levels. Upon analyzing the numerical outputs presented in Figures mentioned above, it becomes evident that the Gradient Descent (GD) algorithm exhibits stability in the presence of noise. It manages to produce reliable results, despite the influence of noise in the measurement data.

However, it is important to note that the gradient descent algorithm algorithm falls short when it comes to capturing the singularities present in the source terms. The numerical outputs in both regular and singular examples do not accurately represent the singularities, suggesting limitations in the algorithm's ability to capture and represent such features.

While the DG algorithm demonstrates stability against noise, its inability to effectively capture the singularities poses a challenge in accurately reconstructing the source terms. This observation highlights the need for further improvements and alternative approaches to address the limitations associated with capturing source singularities.

5.1. Relative error

In this subsection, we present the results of the relative error $Err(f_m)$ with respect to the increasing number of iterations. The relative error serves as a measure of the deviation between the estimated values and the actual values. By examining how the relative error changes as we iterate. To analyze the behavior of the relative error, we systematically increase the number of iterations and monitor the corresponding changes in $Err(f_m)$. This allows us to assess the convergence rate and identify any patterns or trends in the estimation accuracy. The relative error acts as a valuable metric for evaluating the performance of the proposed methods and their ability to approximate the true values of the source term f.



(a) Example 5.1

(b) Example 5.3

Figure 5: The numerical results of the relative error $Err(f_m)$ of a log-type function for the Examples 5.1 and 5.3.

Figures 5 demonstrate the convergence of the relative errors $Err(f_m)$ of a log-type function towards zero in an exponential manner. Upon analyzing the figures, it becomes evident that the relative errors gradually approach the neighborhood of zero. This convergence is observed to follow an exponential pattern, indicating a favorable trend in terms of accuracy improvement with each iteration. The decreasing values of the relative errors suggest that the estimation methods successfully approximate the true values of the source term f as more iterations are performed. These findings reinforce the reliability and effectiveness of the estimation methods employed in our study, ultimately supporting their utility in accurately approximating the source term f through iterative refinement.

6. Conclusion

This paper is devoted to the study of an inverse problem for a time-space fractional diffusion equation. The main objective is to recover a space-dependent source term from noisy final-time observations. First, the existence and uniqueness of the solution to the corresponding direct problem are established through a rigorous theoretical analysis. Subsequently, the inverse problem, which is inherently ill-posed, is reformulated as an optimization problem. Within this framework, we investigate the existence of minimizers together with the uniqueness and stability properties of the minimization problem. To regularize the inverse problem, the classical Tikhonov regularization method is employed, while the resulting approximate solution is computed using a gradient descent algorithm. Finally, several numerical reconstruction experiments in the one-dimensional setting are presented to illustrate the effectiveness, stability, and accuracy of the proposed approach.

References

[1] E. Valdinoci, From the long jump random walk to the fractional laplacian, Boletim da Sociedade Brasileira de Matemática 40 (1) (2009) 33–44.

[2] C. J. Weiss, B. G. van Bloemen Waanders, H. Antil, Fractional operators applied to geophysical electromagnetics, Geophysical Journal International 220 (2) (2020) 1242–1259.

[3] R. Nigmatullin, The realization of the generalized transfer equation in a medium with fractal geometry, Physica status solidi (b) 133 (1) (1986) 425–430.

[4] M. Ruzhansky, D. Serikbaev, B. T. Torebek, N. Tokmagambetov, Direct and inverse problems for time-fractional pseudo-parabolic equations, Quaestiones Mathematicae 45 (7) (2022) 1071–1089.

[5] Z. Li, M. Yamamoto, Inverse problem of a time-space fractional parabolic equation, IMA Journal of Applied Mathematics 84 (3) (2019) 544–566.

[6] S. Dipierro, G. Palatucci, E. Valdinoci, Dislocation dynamics in crystals: a macroscopic theory in a fractional laplace setting, Communications in Mathematical Physics 333 (2015) 1061–1105.

[7] G. M. Viswanathan, V. Afanasyev, S. V. Buldyrev, E. J. Murphy, P. A. Prince, H. E. Stanley, Lévy flight search patterns of wandering albatrosses, Nature 381 (6581) (1996) 413–415.

[8] X. Feng, L. Eldén, M. Yamamoto, Inverse source problem in a space fractional diffusion equation, Inverse Problems 36 (4) (2020) 045008.

[9] E. E. Adams, L. W. Gelhar, Field study of dispersion in a heterogeneous aquifer: 2. spatial moments analysis, Water Resources Research 28 (12) (1992) 3293–3307.

[10] Y. Hatano, N. Hatano, Dispersive transport of ions in column experiments: An explanation of long-tailed profiles, Water resources research 34 (5) (1998) 1027–1033.

[11] A. Kubica, M. Ryter, Time fractional subdiffusion equation with generalized riemann-liouville fractional derivatives, Mathematische Nachrichten 293 (12) (2020) 2319–2345.

[12] Y. Luchko, M. Yamamoto, On the maximum principle for a time-fractional diffusion equation, Fractional Calculus and Applied Analysis 20 (5) (2017) 1131–1145.

[13] A. Oulmelk, L. Afraites, A. Hadri, An inverse problem of identifying the coefficient in a nonlinear time-fractional diffusion equation, Computational and Applied Mathematics 42 (1) (2023) 65.

[14] A. Oulmelk, M. Srati, L. Afraites, A. Hadri, Implementation of the admm approach to constrained optimal control problem with a nonlinear time-fractional diffusion equation, Discrete and Continuous Dynamical Systems - Series S (11 2022). doi:10.3934/dcdss.2022194.

[15] Z. Zhang, Z. Zhou, Numerical analysis of backward subdiffusion problems, Inverse Problems 36 (10) (2020) 105006.

[16] Y. Liu, Z. Li, M. Yamamoto, Inverse problems of determining sources of the fractional partial differential equations, Handbook of fractional calculus with applications 2 (2019) 411–430.

[17] B. Jin, W. Rundell, A tutorial on inverse problems for anomalous diffusion processes, Inverse problems 31 (3) (2015) 035003.

[18] B. Kaltenbacher, W. Rundell, On an inverse potential problem for a fractional reaction–diffusion equation, Inverse Problems 35 (6) (2019) 065004.

[19] Z. Zhang, Z. Zhou, Recovering the potential term in a fractional diffusion equation, IMA Journal of Applied Mathematics 82 (3) (2017) 579–600.

[20] K. Sakamoto, M. Yamamoto, Initial value/boundary value problems for fractional diffusion-wave equations and applications to some inverse problems, Journal of Mathematical Analysis and Applications 382 (1) (2011) 426–447.

[21] W. Rundell, Z. Zhang, On the identification of source term in the heat equation from sparse data, SIAM Journal on Mathematical Analysis 52 (2) (2020) 1526–1548.

[22] J. R. Cannon, Determination of an unknown heat source from overspecified boundary data, SIAM Journal on Numerical Analysis 5 (2) (1968) 275–286.

[23] V. Isakov, Inverse source problems, no. 34, American Mathematical Soc., 1990.

[24] A. Oulmelk, L. Afraites, A. Hadri, M. Nachaoui, An optimal control approach for determining the source term in fractional diffusion equation by different cost functionals, Applied Numerical Mathematics 181 (2022) 647–664.

[25] Y.-K. Ma, P. Prakash, A. Deiveegan, Optimization method for determining the source term in fractional diffusion equation, Mathematics and Computers in Simulation 155 (2019) 168–176.

[26] Y. Li, T. Wei, An inverse time-dependent source problem for a time–space fractional diffusion equation, Applied Mathematics and Computation 336 (2018) 257–271.

[27] A. Kilbas, H. Srivastava, J. Trujillo, Theory and applications of fractional differential equations, North-Holland Mathematics Studies 204 (2006).

[28] G. Acosta, P. Bückle, R. Durán, Finite element approximations for fractional diffusion problems with nonsmooth data, Mathematics of Computation 88 (317) (2019) 979–1003.

[29] D. Murio, Implicit finite difference approximation for time fractional diffusion equations, Computers & Mathematics with Applications 56 (5) (2008) 1138–1145.

[30] P. Zhuang, F. Liu, V. Anh, Implicit runge-kutta method for nonlinear time fractional pdes with delay, SIAM Journal on Numerical Analysis 46 (2) (2008) 1018–1041.